

Whole cell imaging based on wide-field interferometric phase microscopy and its application to cardiomyocytes

Natan T. Shaked*, Lisa L. Satterwhite, Nenad Bursac, and Adam Wax
Department of Biomedical Engineering, Fitzpatrick Institute for Photonics, Duke University
Durham, North Carolina 27708, USA.

*natan.shaked@duke.edu

ABSTRACT

Whole cell imaging is a novel technique using which the time-dependent quantitative phase profiles of live unstained biological cells are analyzed numerically to learn on the cell functionally. Dynamic phase profiles of the sample are first acquired by wide-field digital interferometry (WFDI), a quantitative holographic approach, without the need for scanning or using exogenous contrast agents. The resulting phase profiles are proportional to the multiplication between the cell thickness profile and its integral refractive index profile. However, many morphological parameters, including cell volume and cell force distribution, are based on the cell thickness profile, rather than on its WFDI phase profile. For cells with heterogeneous refractive index structure, more than a single exposure is typically needed to decouple thickness from integral refractive index using the phase profile, with the risk of losing transient acquisition. The presented whole-cell-imaging approach show that the WFDI phase profiles are useful for numerically analyzing cells even in cases where decoupling of thickness and integral refractive index is not possible or desired. We thus define new numerical parameters that directly utilize the WFDI phase profile and demonstrate their usefulness for characterizing contracting cardiomyocytes, cells with complex and highly-dynamic refractive-index structure.

Keywords: Cell analysis, interference microscopy, phase holography, cardiomyocytes.

1. INTRODUCTION

Live biological cells are mostly-transparent three-dimensional objects, and thus imaging them with conventional brightfield light microscopy fails to provide adequate contrast between the cell and its environment. Exogenous fluorescent agents are widely used to enhance the imaging contrast of biological cells, but these agents suffer from photobleaching problem and might be cytotoxic and influence the cellular behavior.

The contrast problem when imaging biological cells can also be solved by using a non-contact, non-invasive phase microscopy, which records the optical path delays (OPDs) of light passing through the cells, and thus obtains information on the cellular structure and dynamics without using any exogenous labeling. The phase of the light that has interacted with the cells needs to be converted to intensity variations for detection since detectors are sensitive to intensity only. This can be performed by phase contrast microscopy and differential interference contrast (DIC) microscopy with a large loss of OPD information. These methods are not inherently quantitative and present distinct imaging artifacts that typically prevent straightforward extraction of the entire OPD profile of the cell.

Wide-field digital interferometry (WFDI) is a label-free holographic technique that is able to record the entire complex wavefront (amplitude and phase) of the light which has interacted with the sample. From the recorded complex field, one can obtain full quantitative OPD profiles of a cell (for each of its spatial points), as well as correct for out-of-focus image features by post-processing. We have applied WFDI microscopy to various types of biological cell systems and recorded a diverse range of cellular phenomena [1-6].

Simple quasi-three-dimensional holographic visualization of the cell phase profile need not be the end of the process. Quantitative analysis should permit extraction of numerical parameters which are useful for cytology or medical diagnosis. Using a transmission-mode interferometric setup, the resulting phase profile represents the multiplication between the refractive index differences and the thickness of the sample. These coupled parameters, the refractive index and the thickness, are not distinct when acquiring the phase profile of a dynamic cell. To allow quantitative cell analysis by WFDI, this fact must be considered during the system development and the following quantitative data analysis.

Many morphological parameters which are useful for cell biologists (such as cell volume, cell force distribution, etc.) are based on the thickness profile of the cell rather than on its phase profile. For cells with homogenous refractive index structure, such as red blood cells, a constant refractive index can be assumed for the entire cell contents and thus the thickness profile can be directly obtained from the WFDI phase profile [7,8]. However, for heterogenous refractive index cells (cells that contain inner organelles with different refractive indices such as cell nucleus and mitochondria), decoupling thickness from refractive index might not be possible by a single exposure WFDI. Multi-exposure methods can be used with the risk of losing dynamic information. For example, decoupling cell refractive index and thickness can be accomplished by measuring the phase profiles of the same cell immersed in two different growth media with distinct refractive indices [9]. Alternatively, when the thickness profile is measured by another method (such as confocal microscopy or atomic force microscopy), it is possible to use the WFDI-based phase profile to calculate the refractive index of the cell inner organelles [10,11].

For highly-dynamic heterogeneous refractive index cells, decoupling of thickness and refractive index using the WFDI phase profiles might not be possible or desired. For these cases, we define new numerical parameters that are based on the dynamic WFDI phase profile of the cells. Experimental demonstrations of this approach are applied to cardiomyocytes (heart muscle cells) undergoing temperature changes. These cells contain a significant number of subcellular organelles with varying refractive indices. The cardiomyocyte dynamics is characterized by a rapid contraction followed by restoration to the resting point. Capturing the dynamics of these heterogeneous refractive-index cells by measuring their phase profiles with WFDI is shown to be a suitable method for obtaining quantitative parameters for biological studies, even without the need to decouple the cell thickness from its refractive index [6].

2. BASIC PRINCIPLES OF WFDI

A possible scheme of a single-exposure WFDI setup is presented in Fig. 1(a). This specific setup is based on Mach-Zehnder interferometer and an off-axis holographic geometry. Light from a coherent source (HeNe laser, for example) is first spatially filtered using a pair of spherical lenses and a confocally-positioned pinhole, and then split into reference and object beams by beam splitter BS₁. The object beam is transmitted through the sample and magnified by a microscope objective. The reference beam is transmitted through a compensating microscope objective (typically similar to the object-beam objective) and then combined with the object beam at an angle. The combined beams are projected onto a digital camera by lens L₂, where the distance between each of the microscope objectives and lens L₂ is equal to the summation of their focal lengths. This configuration allows projection of the amplitude and phase distribution of the sample onto the camera. The combination of the sample and reference beams creates a high-spatial-frequency off-axis hologram of the sample on the digital camera. The digital hologram acquired by the camera is the summation of the object and reference waves, and can be mathematically expressed as follows [12]:

$$H(x, y) = |E_s + E_r|^2 = |E_s|^2 + |E_r|^2 + |E_s| |E_r^*| \exp[j(\phi(x, y) + qx)], \quad (1)$$

where E_s and E_r are respectively the sample and reference field distributions, $\phi(x, y)$ is the spatially-varying phase associated with the sample, q is the fringe frequency due to the angular shift between the sample and reference fields, and x is the coordinate in the direction of the angular shift (assuming linear horizontal fringes in the off-axis hologram).

One of the common digital processing methods applied to the off-axis hologram starts with a digital two-dimensional Fourier transform, where the resulting spatial-frequency contents includes reference-field and sample-field autocorrelations (as a result of transforming the first two elements of Eq. (1)) that are located around the origin of the spatial spectrum, and two mathematically conjugated cross-correlation terms (as a result of transforming the exponential term in Eq. (1)), each located at a different side of the spatial spectrum. The exact locations of the cross-correlation terms are dependent on the angle between the object and reference beams. Looking at the spectrum profile, it is easy to isolate only one of the cross-correlation terms, center it, and perform a digital two-dimensional inverse Fourier transform on the result, yielding $|E_s| |E_r^*| \exp[j(\phi(x, y))]$. Assuming a weak amplitude modulation due to the transparency of the biological cells in culture, the phase argument of the result $\phi(x, y)$ is the phase profile of the sample, for which a phase unwrapping algorithm can be applied to solve 2π ambiguity problems.

As can be seen in Fig. 1(b), presenting the chamber in detail, the *in vitro* cell is typically adhered to the bottom coverslip and is immersed in cell growth medium. The top coverslip of the chamber ensures a constant cell medium height across the chamber and thus a constant physical chamber thickness. Based on this chamber, the spatially-varying phase measured by WFDI is proportional to the OPD profile of the sample and defined as follows:

$$\begin{aligned}
\phi(x, y) &= \frac{2\pi}{\lambda} [\bar{n}_c(x, y) h_c(x, y) + n_m(h_m - h_c(x, y))] \\
&= \frac{2\pi}{\lambda} [(\bar{n}_c(x, y) - n_m) h_c(x, y) + n_m h_m] \\
&= \frac{2\pi}{\lambda} [OPD_c(x, y) + OPD_m],
\end{aligned} \tag{2}$$

where λ is the illumination wavelength, $\bar{n}_c(x, y)$ is the spatially varying integral refractive index, n_m is the medium refractive index, $h_c(x, y)$ is the spatially varying thickness profile of the cell, and h_m is the height of the cell medium. Per spatial point (x, y) , the integral refractive index \bar{n}_c is defined as follows [9]:

$$\bar{n}_c = \frac{1}{h_c} \int_0^{h_c} n_c(z) dz, \tag{3}$$

where $n_c(z)$ is a function representing the intracellular refractive index along the cell thickness. The value of $OPD_m = n_m h_m$ can be measured in advance in places where there are no cells located, and then subtracted from the total OPD measurement. However, $OPD_c = (\bar{n}_c(x, y) - n_m) h_c(x, y)$ contains two coupled parameters: the integral refractive index profile of the cell and the cell thickness profile (under the assumption that n_m is known). These parameters might not be distinct when acquiring the phase profile of a dynamic cell, and this fact must be considered during development of the WFDI optical system capturing the cell phase profile and in the quantitative data analysis that follows. Local changes in the cell refractive index along the cell thickness may occur during various dynamic processes, such as action potential propagation, or by transverse movement of the inner organelles of the cell. Independently or not, thickness changes can occur due to any morphological change of the cell such as membrane fluctuations and cell swelling.

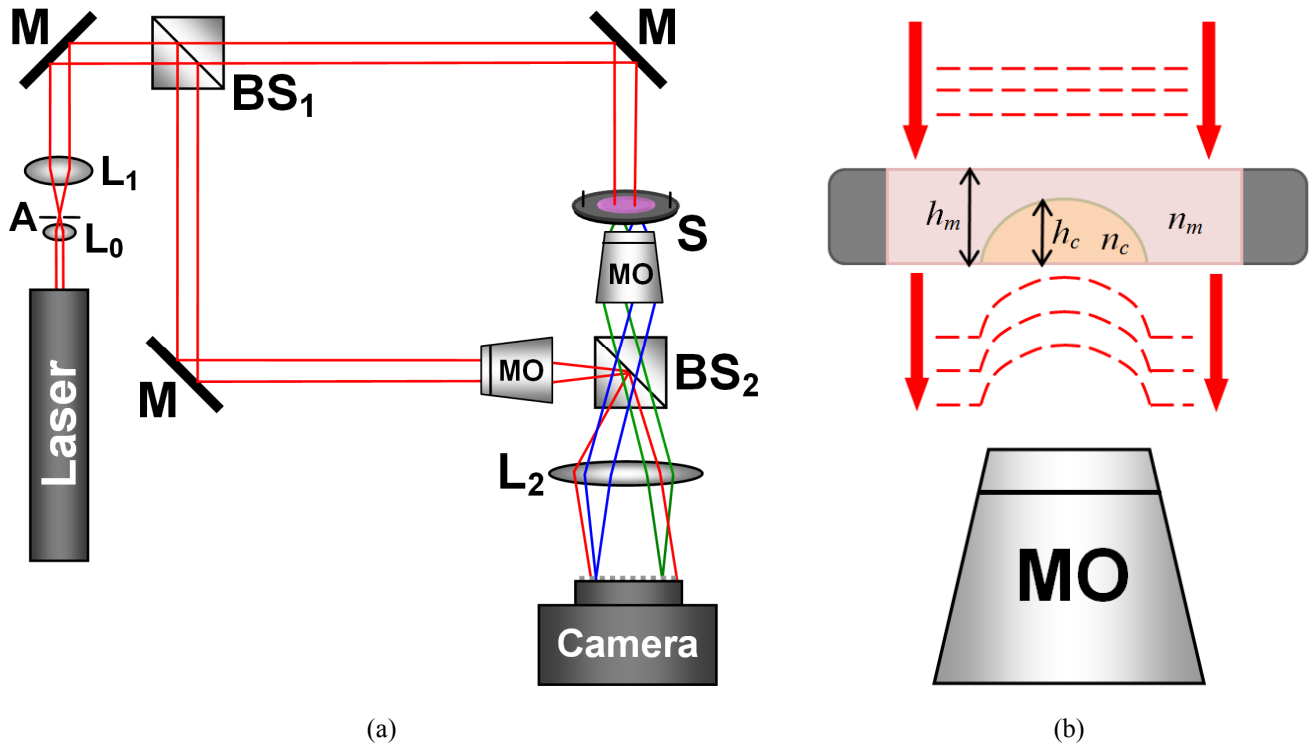


Fig. 1. (a) Off-axis WFDI phase-microscopy system. A = Pinhole; L_0, L_1, L_2 = Lenses; BS_1, BS_2 = Beam splitters; M = Mirror; S = Sample; MO = Microscope objective; (b) Detailed scheme of the sample chamber [12].

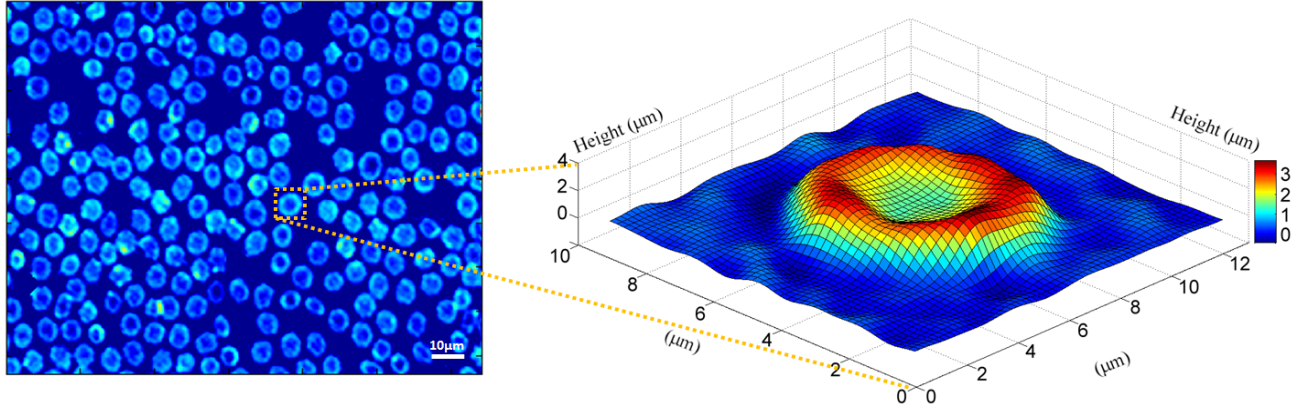


Fig. 2. WFDI phase profile of rat whole blood, demonstrating the valuable quantitative morphological data that can be obtained by WFDI in a single exposure and without any type of sample preparation or labelling. Cell height (thickness) profile is shown on the right. This quantitative profile can be derived for each cell in the FOV [12].

For homogenous refractive index cells, such as mature red blood cells, for which a constant refractive index can be assumed for the entire cell contents, the thickness profile can be directly obtained from the phase profile [7,8]. Figure 2 shows the phase profiles of rat red blood cells obtained by WFDI in our laboratory, and the associated thickness profile for an arbitrary cell in the field of view (FOV). Note, however, that this approach of decoupling cell thickness from refractive index in WFDI phase profiles is limited to homogeneous cell types that do not contain nuclei or other organelles with varying refractive indices.

Other studies [13,14] have shown that for heterogeneous cells that contain organelles with different refractive indices, certain parameters such as cell area and dry mass can be obtained directly from the phase profile. In addition, if the cell volume transiently increases in an isotropic way (for example, due to swelling), relative volume can still be calculated in a good approximation. For example, we have shown that cell swelling in articular chondrocytes can be analyzed quantitatively by WFDI [4].

3. ANALYSING THE DYNAMIC WFDI PHASE PROFILE

To be able to analyze the WFDI phase profile directly, without the need to decouple thickness and refractive index, we have proposed the following analysis [6]. We first define the phase-average displacement (PAD) as follows:

$$\Delta\varphi_t(x, y) = \varphi_t(x, y) - \varphi_0(x, y), \quad (4)$$

where $\varphi_t(x, y)$ is the spatially varying phase at time point t , and $\varphi_0(x, y)$ is the spatially varying phase at the resting time point of the cell, or, if such time point is not known $\varphi_0(x, y)$ is defined as the time average of the entire phase-profile transient $\varphi_0(x, y) = \langle \varphi_t(x, y) \rangle_t$. Using Eq. (4), we define the positive and negative mean-square phase-average displacements (MS-PAD⁺ and MS-PAD⁻, respectively) as follows:

$$\begin{aligned} \Delta\varphi_{MS}^+(x, y) &= \left\langle (\Delta\varphi_t(x, y))^2 : \Delta\varphi_t(x, y) \geq 0 \right\rangle_t, \\ \Delta\varphi_{MS}^-(x, y) &= \left\langle (\Delta\varphi_t(x, y))^2 : \Delta\varphi_t(x, y) < 0 \right\rangle_t, \end{aligned} \quad (5)$$

and the spectral-domain MS-PAD as follows:

$$\Delta\varphi_{MS}(f_x, f_y) = \left\langle |\Delta\varphi_t(f_x, f_y)|^2 \right\rangle_t, \quad (6)$$

where $\Delta\varphi_t(f_x, f_y)$ is obtained by a spatial Fourier transform of $\Delta\varphi_t(x, y)$. Using Eqs. (5) and (6), we define the following parameters to describe the MS-PAD global contributions:

$$\eta_1^+ = \sqrt{\langle \Delta\varphi_{MS}^+(x,y) \rangle_{(x,y)}}, \quad \eta_1^- = \sqrt{\langle \Delta\varphi_{MS}^-(x,y) \rangle_{(x,y)}}, \quad \eta_2 = \sqrt{\langle \Delta\varphi_{MS}(f_x, f_y) \rangle_{(f_x, f_y)}}, \quad (7)$$

where $\langle \bullet \rangle_{(x,y)}$ and $\langle \bullet \rangle_{(f_x, f_y)}$ define an area averaging.

Let us also define the phase instantaneous displacement (PID) as follows:

$$\Delta\varphi_{t,\tau}(x,y) = \varphi_{t+\tau}(x,y) - \varphi_t(x,y), \quad (8)$$

where τ defines the time duration between time point t and time point $t + \tau$. Using Eq. (8), we define the positive and negative mean-square phase instantaneous displacements (MS-PID⁺ and MS-PID⁻, respectively) as follows:

$$\begin{aligned} \Delta\varphi_{MS,\tau}^+(x,y) &= \langle (\Delta\varphi_{t,\tau}(x,y))^2 : \Delta\varphi_{t,\tau}(x,y) \geq 0 \rangle_t, \\ \Delta\varphi_{MS,\tau}^-(x,y) &= \langle (\Delta\varphi_{t,\tau}(x,y))^2 : \Delta\varphi_{t,\tau}(x,y) < 0 \rangle_t, \end{aligned} \quad (9)$$

as well as the spectral-domain MS-PID as follows:

$$\Delta\varphi_{MS,\tau}(f_x, f_y) = \langle |\Delta\varphi_{t,\tau}(f_x, f_y)|^2 \rangle_t, \quad (10)$$

where $\Delta\varphi_{t,\tau}(f_x, f_y)$ is obtained by a spatial Fourier transform of $\Delta\varphi_{t,\tau}(x,y)$. By using Eqs. (9) and (10), we define parameters describing the MS-PID global contributions:

$$\gamma_{1,\tau}^+ = \sqrt{\langle \Delta\varphi_{MS,\tau}^+(x,y) \rangle_{(x,y)}}, \quad \gamma_{1,\tau}^- = \sqrt{\langle \Delta\varphi_{MS,\tau}^-(x,y) \rangle_{(x,y)}}, \quad \gamma_{2,\tau} = \sqrt{\langle \Delta\varphi_{MS,\tau}(f_x, f_y) \rangle_{(f_x, f_y)}}. \quad (11)$$

Since the cell phase profile is strongly associated with its dry mass [13,14], the parameters defined above are associated with motion of different cell structures including subcellular organelles. Note that all the parameters defined above are based on the entire phase-profile transient, without the need to extract the thickness profile first.

The presented analysis tools are sensitive enough to detect the subtle changes in the dynamic phase profile of beating cardiomyocytes (heart-muscle cells) [6]. Figures 3(a) and (e) compare the phase profiles of a cardiomyocyte during a

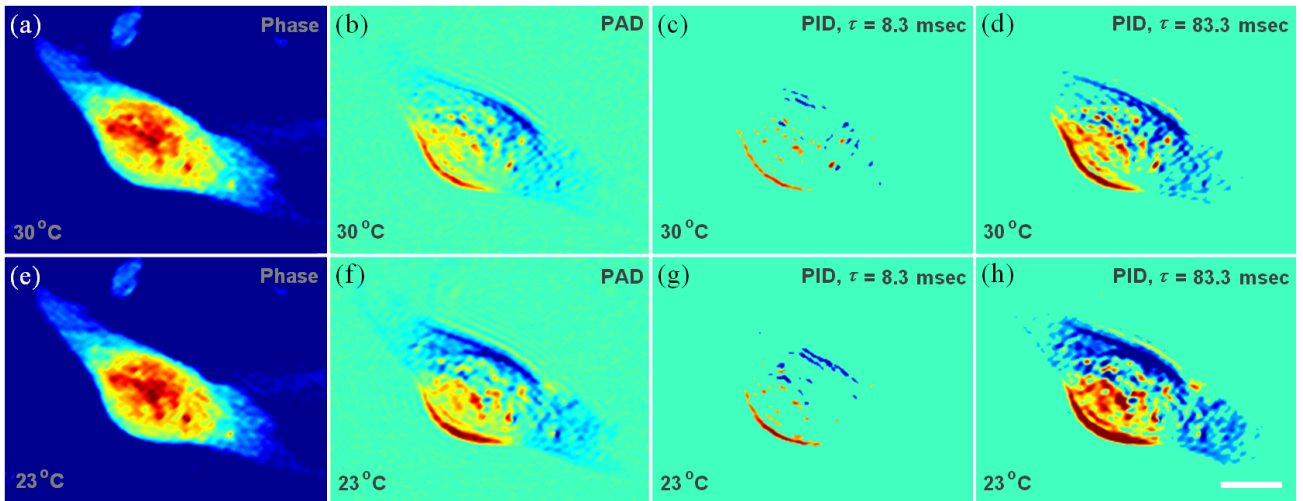


Fig. 3. Example of numerical analysis applied on a WFDI phase profile of a cardiomyocyte during beating at two different temperatures: (a-d) at 30°C, (e-h) at 23°C. (a,e) Phase profile; (b,f) PAD profile; (c,g) PID profile for $\tau = 8.3$ msec; (d,h) PID profile for $\tau = 83.3$ msec. In (b-d,f-h): 'hot' colors represent positive values, 'cold' colors represent negative values, and cyan represents zeros. White horizontal scale bar represents 10 μm [6]. Dynamics, 120 fps for 1 sec: Media 4 in Ref. [6].

single beating cycle at 30°C and 23°C, respectively. The cell in Fig. 3(e) shows more motion along a greater portion of its length in comparison to the cell shown in Fig. 3(a), especially in the recovery stage (the time interval between the point of maximum stretch of the cell and the point when the cell returned to the resting stage). The dynamic differences during the beating cycle of the same cell at 30°C in comparison to 23°C are more obvious from the PAD and PID profiles shown in Figs. 3(b-d,f-h) (see also Media 4 in [6]). As seen in these figures, the PAD and PID profiles provide a means of tracking the differential changes in the dynamic WFDI phase profile, which reveal the dry-mass movement in the cell associated with organelles of different sizes over different time periods during the cell dynamics.

The numerical analysis described above was performed on the WFDI phase profiles of 18 individual cardiomyocytes at 30°C and then repeated at 23°C [6]. The values obtained for each of the γ and η parameters were averaged over 3-4 beating cycles and normalized by the viewable area of the cell. Figure 4 summarizes the results obtained. Statistical significance between the two groups of cells (at 30°C and at 23°C) were seen for all γ and η parameters as indicated by low p -values (which were calculated by the two-sided Wilcoxon rank-sum test). These results demonstrate that the unique whole-cell-based numerical parameters can be used to discriminate between different dynamic behaviors of cardiomyocytes, and thus can be used to quantitatively study the dynamic phenomena in these cells.

As can also be seen in Fig. 4, there is an apparent advantage for using the negative parameters $\gamma_{1,\tau}^-$ for discriminating between the two groups of cells. Higher values in these parameters represent increased levels of MS-PID-. In the recovery phase of the cell, it is more likely to have more cell points with negative MS-PID than positive MS-PID, since the phase profile in the cell contractile region decreases. This implies that there is a larger influence of the ambient temperature in the recovery phase of the cell beating, as compared to the contraction phase. These results are supported by previous studies performed by other methods, where temperature had a profound effect on the biochemistry of contraction in the myocardium of the intact heart and in cardiomyocytes *in vitro* [15].

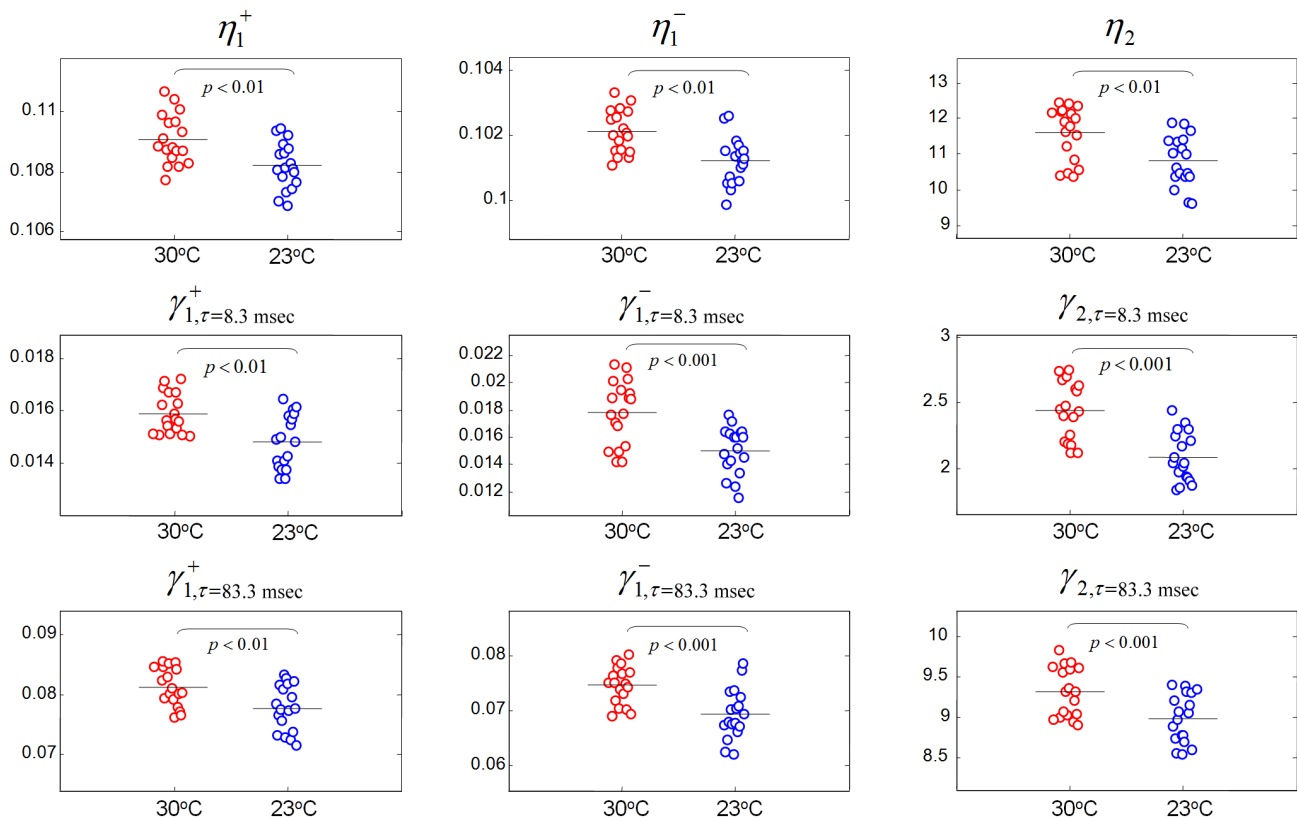


Fig. 4. Values of the γ and η parameters that are based on the whole-cell phase profiles, demonstrating that these parameters discriminate between cardiomyocytes beating at 30°C and 23°C (18 cells in each group, 3-4 beating cycles per each cell). Each circle represents a different cardiomyocyte, and the horizontal line at each group represents the average value for all cells in the group [6].

4. CONCLUSIONS

We have presented whole-cell analysis tools that are directly based on the dynamic WFDI phase profile of the cell, without the need to decouple refractive index from thickness. The utility of the defined parameters is demonstrated for beating cardiomyocytes. We have shown that the technique is sensitive enough to capture intermediate events associated with dry mass movement over different time scales during the cardiomyocyte beating cycle in different temperatures. These intermediate events cannot be well discriminated by directly visualizing the dynamic WFDI phase profiles of the cell. In contrast, the single-valued η and γ parameters can uniquely characterize cell function in certain environmental conditions. We believe that these numerical tools will be useful for analyzing various fast dynamic behaviors in biological cells, including intracellular and extracellular membrane fluctuations and reorganization of the cell cytoskeleton. More details on this subject including additional experimental results can be found in Ref. [6].

ACKNOWLEDGMENTS

This work was supported by National Science Foundation (NSF) grant CBET-0651622. N.T.S. greatly acknowledges the support of the Bikura Postdoctoral Fellowship from Israel.

REFERENCES

- [1] Shaked, N. T., Rinehart, M. T. and Wax, A., "Dual-interference-channel quantitative-phase microscopy of live cell dynamics," *Opt. Lett.* 34, 767-769 (2009).
- [2] Shaked, N. T., Zhu, Y., Rinehart, M. T. and Wax, A., "Two-step-only phase-shifting interferometry with optimized detector bandwidth for microscopy of live cells," *Opt. Express* 17, 15585-15591 (2009).
- [3] Shaked, N. T., Newpher, T. M., Ehlers, M. D. and Wax, A., "Parallel on-axis holographic microscopy of biological cells and unicellular micro-organism dynamics," *Appl. Opt.* 49, 2872-2878, (2010).
- [4] Shaked, N. T., Finan, J. D., Guilak, F. and Wax, A., "Quantitative phase microscopy of articular chondrocyte dynamics by wide-field digital interferometry," *J. Biomed. Opt. Lett.* 15, 010505 (2010).
- [5] Shaked, N. T., Zhu, Y., Badie, N., Bursac, N. and Wax, A., "Reflective interferometric chamber for quantitative phase imaging of biological sample dynamics," *J. Biomed. Opt. Lett.* 15, 030503 (2010).
- [6] Shaked, N. T., Satterwhite, L. L., Bursac, N. and Wax, A., "Whole cell analysis of live cardiomyocytes using wide-field interferometric phase microscopy," *Biomed. Opt. Express* 1, 706-719 (2010).
- [7] Popescu, G., Ikeda, T., Badizadegan, K., Dasari, R. R. and Feld, M. S., "Erythrocyte structure and dynamics quantified by Hilbert phase microscopy," *J. Biomed. Opt. Lett.* 10, 060503 (2005).
- [8] Rappaz, B., Barbul, A., Emery, Y., Korenstein, R., Depeursinge, C., Magistretti, P. J. and Marquet, P., "Comparative study of human erythrocytes by digital holographic microscopy, confocal microscopy, and impedance volume analyzer," *Cytometry* 73A, 10, 895-903 (2008).
- [9] Rappaz, B., Marquet, P., Cuche, E., Emery, Y., Depeursinge, C. and Magistretti, P., "Measurement of the integral refractive index and dynamic cell morphometry of living cells with digital holographic microscopy," *Opt. Express* 13, 9361-9373 (2005).
- [10] Curl, C. L., Bellair, C. J., Harris, T., Allman, B. E., Harris, P. J., Stewart, A. G., Roberts, A., Nugent, K. A. and Delbridge, L. M., "Refractive index measurement in viable cells using quantitative phase-amplitude microscopy and confocal microscopy," *Cytometry* 65A, 88-92 (2005).
- [11] Edward, K., Farahi, F. and Hocken, R., "Hybrid shear force feedback/scanning quantitative phase microscopy applied to subsurface imaging," *Opt. Express* 17, 18408-18418 (2009).
- [12] Shaked, N. T., Satterwhite, L. L., Rinehart, M. T. and Wax, A., "Quantitative analysis of biological cells using digital holographic microscopy," in [Holography, Research and Technologies], INTECH (2011).
- [13] Popescu, G., Park, Y. K., Lue, N., Best-Popescu, C. A., Deflores, L., Dasari, R. R., Feld, M. S. and Badizadegan, K., "Optical imaging of cell mass and growth dynamics," *Am. J. Physiol. Cell Physiol.* 295, C538-544 (2008).
- [14] Rappaz, B., Cano, E., Colomb, T., Kühn, J., Simanis, V., Depeursinge, C., Magistretti, P.J. and Marquet, P., "Noninvasive characterization of the fission yeast cell cycle by monitoring dry mass with digital holographic microscopy," *J. Biomed. Opt.* 14, 034049 (2009).
- [15] Fu, Y., Zhang, G.-Q., Hao, X.-M., Wu, C.-H., Chai, Z. and Wang, S.-Q., "Temperature dependence and thermodynamic properties of Ca^{2+} sparks in rat cardiomyocytes," *Biophysical Journal* 89, 2533-2541 (2005).